Preprint Title In vitro effect of hyperthermic Ag and Au Fe_3O_4 nanoparticles in cancer cells

Authors Hector Katifelis, Iuliia Mukha, Anna Lyberopoulou, Nadiia Vityuk, Matina Grammatikaki, Ievgen Pylypchuk, Foivos Lazaris, Liudmyla Storozhuk, Vassilios Kouloulias and Maria Gazouli

Publication Date 09 Sep 2019

Article Type Full Research Paper

ORCID® iDs Vassilios Kouloulias - https://orcid.org/0000-0003-2082-7323; Maria Gazouli - https://orcid.org/0000-0002-3295-6811

In vitro effect of hyperthermic Ag and Au Fe_3O_4 nanoparticles in cancer cells

Hector Katifelis[1], Iuliia Mukha[2], Anna Lyberopoulou[1], Nadiia Vityuk[2], Matina Grammatikaki[1], Ievgen Pylypchuk[2], Foivos Lazaris[1], Liudmyla Storozhuk[2], Vassilios Kouloulias[3], Maria Gazouli[1,3]

Address: [1]Laboratory of Biology, Medical School, National and Kapodistrian, University of Athens, Michalakopoulou 176, Athens, 11527, Greece, [2]Chuiko Institute of Surface Chemistry, NAS of Ukraine, 17 General Naumov Kyiv, 03164, Ukraine, [3]2nd Department of Radiology, Radiotherapy Unit, Medical School, National and Kapodistrian University of Athens, ATTIKON University Hospital, Rimini 1 Chaidari, Athens, 12462, Greece

Email: Maria Gazouli* - mgazouli@med.uoa.gr

* Corresponding author

Abstract

Metal nanoparticles (NPs) in cancer management have gained great attention the last decade. However, research is needed regarding the targeting potential, the therapeutic effects, in vitro/vivo stability and their cytotoxic effects in order to be successfully incorporated in the clinical practice. In this study, we investigated the anti-cancerous effect of hyperthermic Fe_3O_4 core Ag(Au) $_{shell}$ NPs constructed with tryptophan as stabilizer and reducing agent. Both NPs have toxic effects after ionization, working as hyperthermic NPs. The toxic effect of hyperthermic NPs is minimized in non-cancerous HEK293 cells. We also studied the expression of hsp-70, bcl-2 and casp-3 in HEK293, HCT116, 4T1 and HUH7 cells and the expression of p53 in HEK293, HCT116 and HUH7. Our results show that Fe_3O_4 $_{core}$ Ag(Au) $_{shell}$ NPs induce apoptosis; 4T1 cells also undergo apoptosis via a p53-independent pathway. However, the role of tryptophan regarding the reduced toxic effects in non-cancerous cells requires further investigation.

Keywords

anti-tumour effect; Fe_3O_4 $_{core}$ Ag(Au) $_{shell}$ nanoparticles; hyperthermia; magnetic nanoparticles; tryptophan

Introduction

Hyperthermia refers to the type of treatment in which body tissue is exposed to high temperature in order to damage and kill cancer cells or make them more sensitive to radiation and anticancer drugs [1,2]. Different tools have been suggested to induce hyperthermia such as ionizing radiation, laser and microwaves to heat up malignant tissues. Radiotherapy and chemotherapy have been widely used in tumour regions but leading to harmful effects on healthy tissues [2]. Although these approaches are able to increase the intracellular temperature up to cancer cell death, they can also inflict damage at healthy tissues [2,3].

Therefore, nanotechnology has come with a novel solution to this problem providing an alternative of non-invasive techniques with the use of different kinds of nanoparticles (NPs) as heating mediators. An increasing number of reviews about noble metal NPs in cancer management indicates a growing interest to these promising nanoobjects. Gold and silver NPs can be applied on their own or in combination with other molecules (i.e., polymers, surfactants, organic dyes) for targeting, imaging and therapeutics [4]. In particular, hyperthermic NPs are proven to be a promising tool in cancer therapy. In magnetic hyperthermia, magnetically active NPs like Fe_3O_4 NPs, absorb energy and convert it into heat (>41,5^{o}C). Magnetic NPs have been successfully used in many studies and even progressed in clinical trials [5,6]. However, in order to succeed a specific anti-tumour effect to the tumour site, the construction of targeted NPs seems compulsory.

Previously, we estimated the nanotoxicity of colloidal mono- and bimetallic silver/gold NPs stabilized with amino acid tryptophan (Trp), in three different cell lines 4T1, a breast cancer cell line, HCT116, a colon cancer cell line and HEK293, embryonic kidney cell line [7]. Among other results, we found that the toxicity of NPs was

essentially lower in non-cancerous cells, making them promising candidates as tools for cancer treatment approaches [7,8]. Thus, in this study we wanted to check the effect of hyperthermic Fe_3O_4 $_{core}$ Ag(Au) $_{shell}$ NPs in cancer cell cultures. Our initial hypothesis is that cancer cell lines exposed to hyperthermic NPs will receive thermal damage which will lead to cellular death. In order to test this hypothesis, we included a fourth cell line, HUH7 a well differentiated hepatocyte derived cellular carcinoma and we also approached the potential molecular mechanism underlying in vitro hyperthermia in cancer cells. Thus, we estimated the expression profile of genes involved programmed cell death (casp-3, p53, bcl-2) and hsp-70, an essential gene for cellular responses to environmental stressors including hyperthermia [9]. These hyperthermic NPs are stabilized with amino acid tryptophan as an effective way in attenuating potential hepatotoxicity and nephrotoxicity of NPs during their future in vivo application [10].

Results

Characterization of magnetic NPs

Prepared colloidal solutions of magnetic NPs containing iron oxide core and noble metal shell had a bright yellow and red colour inherent to NPs of silver and gold respectively.

A specific colour is a distinguishing feature of noble metal NPs and is caused by the phenomenon of localized surface plasmon resonance (LSPR) that appears as absorption in the visible range of the spectrum. The maxima of LSPR absorption bands of Fe_3O_4 $_{core}$ Ag $_{shell}$ and Fe_3O_4 $_{core}$ Au $_{shell}$ colloids were localized at 420 and 527 nm (Figure 1), indicating the formation of continuous shell around the magnetite particles. Obtained NPs, with both silver and gold shell, were of spherical shape with

the average size of 10-20 nm according to data obtained by transmission electron microscopy (TEM) and dynamic light scattering (DLS) methods (Figure 1). Both colloids carried neutral pH, namely 7,2 for Fe_3O_4 core Au shell and 7,7 for Fe_3O_4 core Ag shell.

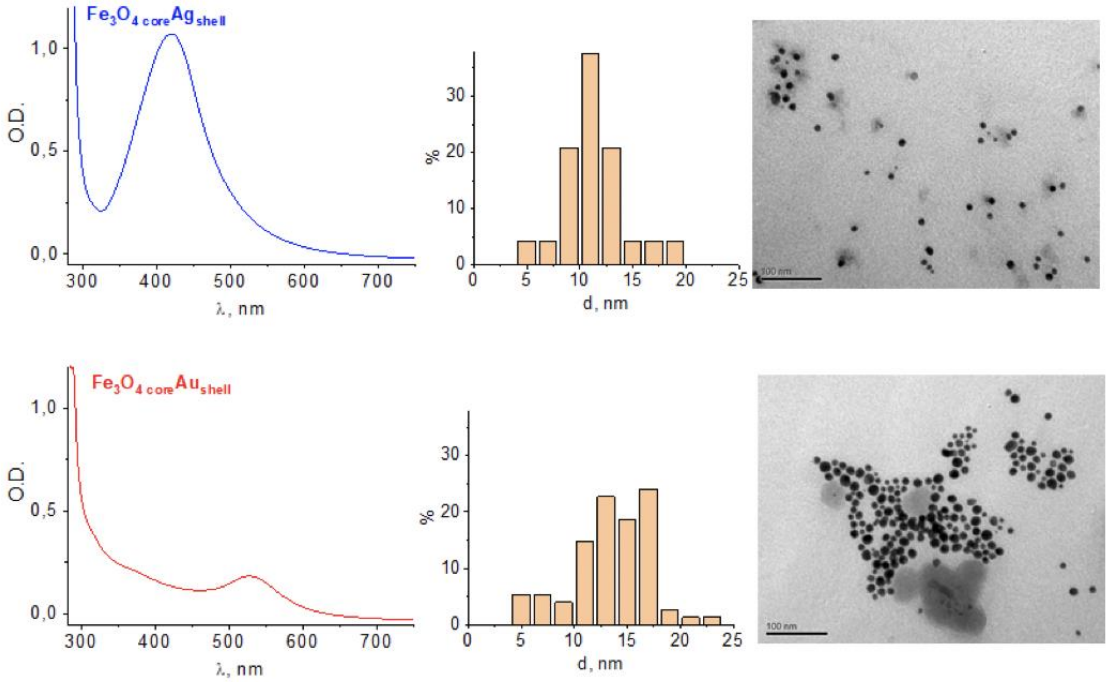

Figure 1: Properties of Fe_3O_4 core Ag(Au) shell nanoparticles. Absorbance spectra of magnetic nanoparticles with the shell of silver (top) and gold (bottom) with corresponding TEM images and size distribution calculated with ImageJ.

Hyperthermic-NPs induced toxicity

Fe_3O_4 core Ag shell, Fe3O4 core Au shell and Fe_3O_4 NPs were tested regarding their toxicity under hyperthermic and non-hyperthermic conditions (concentrations used 200, 400 and 600µg/mL). The MTT results are shown in bar diagrams for HEK293 (Figure 2a),

HCT116 (Figure 2b), 4T1 (Figure 2c) and HUH7 (Figure 2d) cell lines. Based on our results the largest decrease in viability between ionized and non-ionized cells is found on HCT116 cells (concentrations 400μg/mL and 600μg/mL of Fe_3O_4 core Au shell NPs led to a decrease in viability approximately 40 and 55% respectively). Fe_3O_4 core Au shell NPs appear highly toxic for 4T1 cells; while non-ionized 4T1 cells show a low, dose-independent toxicity (approximately 80% viability) ionized cells show a decrease of viability by 58 and 65% (for concentrations 400μg/mL and 600μg/mL). In HUH7 cells, there is approximately 30% difference of viability between ionized and non-ionized cells incubated with Fe_3O_4 core Ag shell. (concentrations 200, 400 and 600μg/mL) Interestingly, in 400 and 600μg/mL of hyperthermic of hyperthermic Fe_3O_4 core Au shell and in 200 and 400μg/mL of with Fe_3O_4 core Ag shell the toxic effects of these NPs are reduced in non-cancerous cells, HEK293 (Fig 2a).

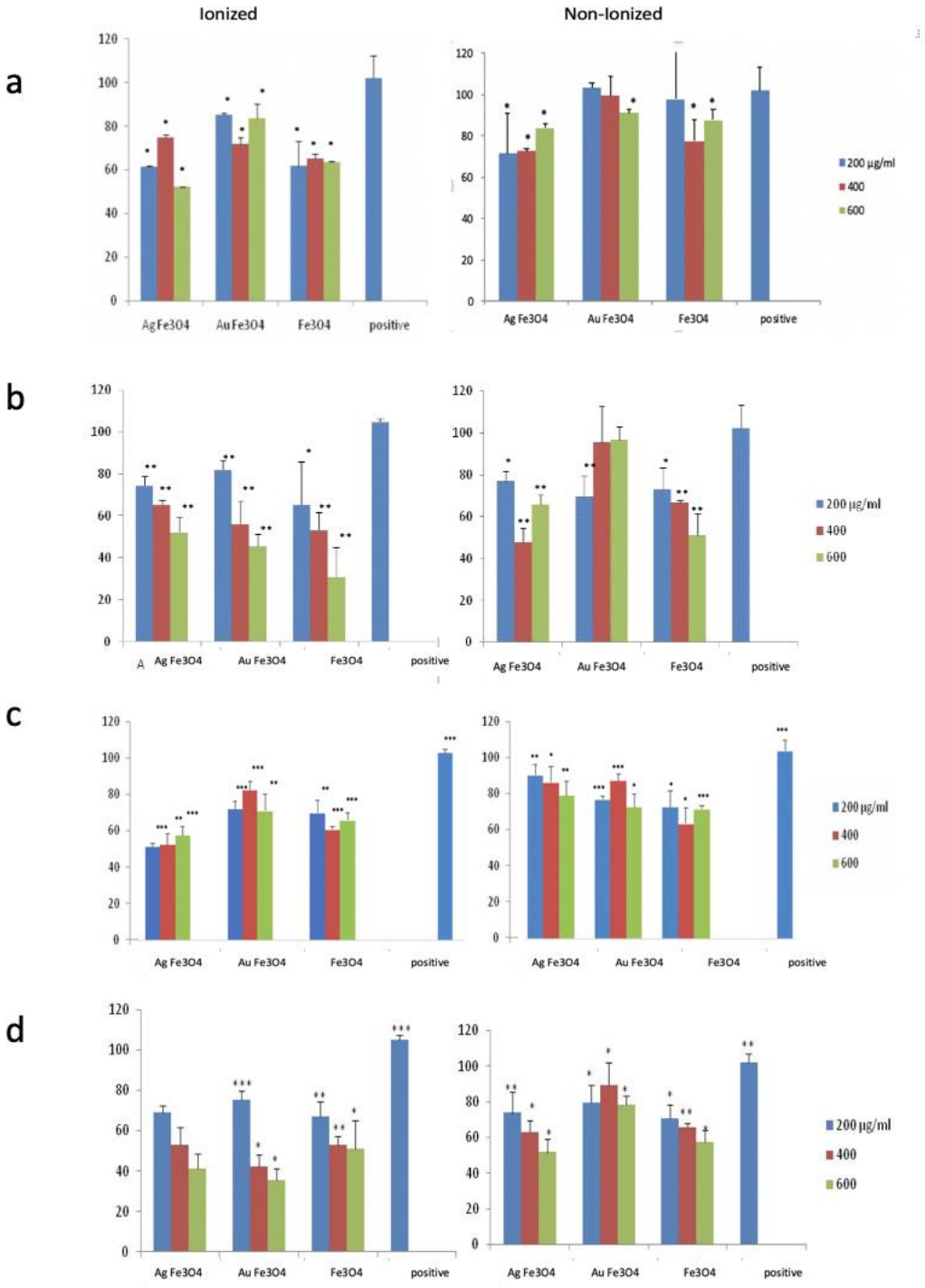

Figure 2: Viability assay on cell lines. Graph of MTT assay after treatment with various NPs of different concentrations of Fe_3O_4 a) on HEK293 and b) HCT116 c) 4T1 d) HUH7 and subsequent ionization (graphs on the left). Non-ionized cells (graphs on the right) were used as control plates. Positive control shows cells without

the exposure of NPs. The cell viability is expressed as % cell viability ±SD between two experiments. The symbols *, **, *** show statistical significance using one-way ANOVA ($p<0,05$, $p<0,01$, $p<0,005$ respectively) compared to the positive control.

Effect of hyperthermic NPs on hsp-70 and apoptotic genes

Quantitive real-time PCR was performed to analyse the mRNA levels of hsp-70, bcl-2 and casp-3 in HEK293, HCT116, 4T1 and HUH7 cells and p53 in HEK293, HCT116 and HUH7 (concentration 400μg/mL of all three NPs tested). In ionized HEK293 cell line, Fe_3O_4 $_{core}$ Ag $_{shell}$ did not change the expression of the genes tested (Figure 3a). Fe_3O_4 $_{core}$ Au $_{shell}$ led to the up-regulation of hsp-70 and a mild up-regulation of casp-3; bcl-2 was down-regulated while p53 remained unaffected. Fe_3O_4 slightly down-regulated p53 and bcl-2 with no effect on hsp-70. Casp-3 expression remained almost unchanged. In ionized HCT cells hsp-70, p53 and casp-3 were up-regulated in all three NPs; bcl-2 was down-regulated (Figure 3b). Similarly, ionized 4T1 cells showed up-regulation of hsp-70 and casp-3; bcl-2 was down-regulated for Fe3O4 core Au shell and Fe_3O_4 but remained unchanged for Fe_3O_4 $_{core}$ Ag $_{shell}$. p53 expression was not calculated since as already mentioned 4T1 cells are p53 null (Figure 3c). Finally, HUH7 cells showed an up-regulation of p53, casp-3 and mild up-regulation for hsp-70 while bcl-2 was down-regulated for Fe_3O_4 $_{core}$ Ag $_{shell}$ but its levels remained almost unchanged for Fe_3O_4 $_{core}$ Au $_{shell}$ and Fe_3O_4 (Figure 3d).

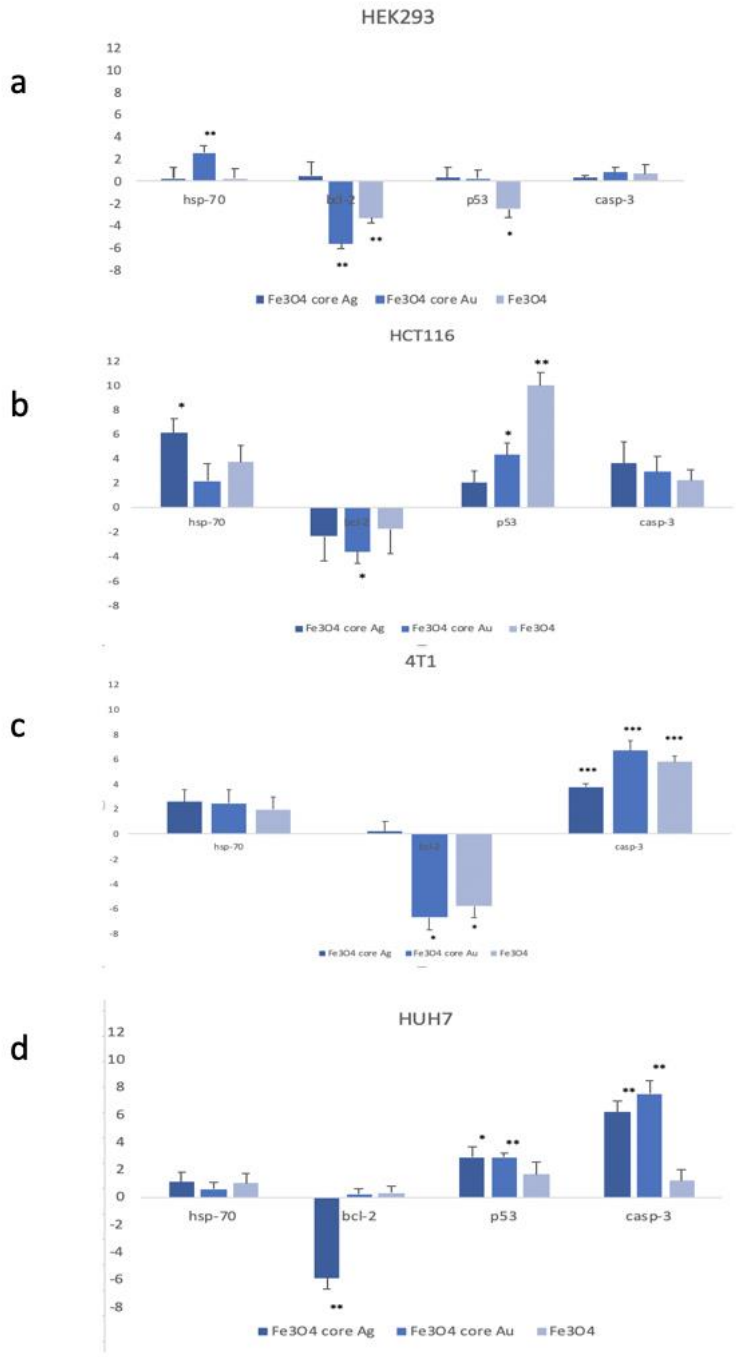

Figure 3: Fold change of hsp-70, bcl-2, p53 and casp-3 in ionized a) HEK293, b) HCT116, c) 4T1 and d) HUH7 cells with 400µg/mL of Fe_3O_4 $_{core}$ Ag $_{shell}$, Fe_3O_4 $_{core}$ Au $_{shell}$ and Fe_3O_4 nanoparticles.

Discussion

According to our results, the NPs that have a toxic effect towards cancer cells after ionization, and thus work as hyperthermic NPs, are Fe_3O_4 core Au shell NPs in the concentrations 400 and 600 μg/ml of Fe_3O_4, in both 4T1 and HCT116 cell lines (Figures 2b, c). Specifically, non-ionized HCT116 show no toxicity in concentrations 400 and 600 μg/ml of Fe_3O_4 (~5% toxicity), while in 200 μg/ml of Fe_3O_4 the toxicity is ~30%. On the other hand, ionized HCT116 in concentrations 400 and 600 μg/ml of Fe_3O_4 show ionization-dependent toxicity (40% and 55% respectively). In 200 μg/ml of Fe_3O_4 the toxicity is no ionization-dependent.

Regarding non-ionized 4T1, they show maximum 20% toxicity in the three concentrations tested, opposed to ionized 4T1 that in the concentrations 400 and 600 μg/ml of Fe_3O_4 show high toxicity (~58% and 65% respectively), indicating ionization-dependent toxicity. Fe_3O_4 core Ag shell NPs because of the toxic effect of Ag NPs on their own, compared to Au NPs that are considered to be the less toxic metal NPs for in vivo applications, do not seem to act as heating mediators [7,14]. Fe_3O_4 core Ag shell NPs show no ionization-dependent toxicity in both cell lines. Interestingly, in the same concentrations the toxic effect of hyperthermic Fe_3O_4 core Au shell NPs is minimized in non-cancerous cells HEK293 (Figure 2a) VS ~55% viability in cancer cells with 400μg/ml and 45% viability with 600μg/ml) (Figures 2 a-c).

On the contrary, it is Fe_3O_4 core Ag shell NPs that show a decrease of viability in HUH7 cells, serving as hyperthermia-inducing agents whereas both Fe_3O_4 core Au shells and Fe_3O_4 have a lower cytotoxic effect. Ag NPs show a dose-independent toxicity with almost 30% difference between ionized and non-ionized cells in all three concentrations tested. Thus, it seems that there is not a single hyperthermic NPs suitable for all cancer cell types but different hyperthermic NPs are cytotoxic for

different cancer cells. Furthermore, as already mentioned, Ag NPs have an endogenous toxicity that Au NPs lack. This finding suggests that hyperthermia and Ag could have a synergistic effect on HUH cells; neither non ionized HUH7 cells incubated with Fe_3O_4 $_{core}$ Ag $_{shell}$ nor bare Fe_3O_4 on ionized HUH7 show similar toxicity. Therefore, these results indicate that HUH7 could be hyperthermia-resistant, requiring the action of Ag for toxicity to be induced. Indeed, increased resistance to hyperthermia has already been described in a study [15] in which integrin-linked kinase was associated with poor response to hyperthermia. However, the molecular basis of this phenomenon remains unclear.

Moving a step forward, we examined the expression profiles of hsp-70 and genes with a key role in apoptosis (p53, casp-3 and bcl-2). Hsp-70 is a protein family induced under environmental stress, heat shock included during which they assist the cell to cope with increased levels of denaturated proteins and prevent apoptosis. Considered as the hallmark of hyperthermia, up-regulation of hsp-70 in exposed cells is found in several studies [16,17]. Hsp-70 serves as a danger signal by triggering immunological responsiveness towards cancer cells and increasing tumour tissue infiltration by eosinophil granulocytes [18]. Tsang et al [19], reported that administration of both hsp-70 and dendritic cells at irradiated cancer tissue triggers a more potent anti-cancer tumour response than dendritic cells alone. In our study, except Fe_3O_4 $_{core}$ Au $_{shell}$ NPs, ionized HEK293 show almost no fold change in hsp-70 expression, suggesting a lower intake of hyperthermic NPs. On the other hand, HUH7 had a mild up-regulation of hsp-70. Combined with the MTT results, this finding supports the synergistic hypothesis (hyperthermia combined with Ag result in increased toxicity); hyperthermia alone mildly affected the viability of HUH7 cells. HCT116 and 4T1 cells showed the highest up-regulation of hsp-70 in all four cell

lines and also showed a high decrease in viability (ionized HCT116 and 4T1 using Fe_3O_4 core Au shell NPs, 400μg/mL).

Following the study of hsp-70 fold change, our next goal was to approach the molecular pathway that leads to cancer cell death. Apoptosis is of crucial importance for cell fate since pro and antisurvival signals determine tumour initiation and progression. However, cancer cells are apoptosis-resistant while many chemotherapeutic drugs function by triggering apoptotic mechanisms [20]. P53 is a tumour suppressing gene that guards genome and inhibits tumorigenesis since it promotes DNA repair and cell death [21]. Bcl-2 is anti-apoptotic gene, targeted by p53 transcription factor and promotes cell survival by binding cytochrome C residues. Casp-3 also has a key-role in apoptosis by catalysing the cleavage of several important intracellular proteins [22-24].

In our study, p53 and casp-3 were found up-regulated, except HEK293 cells where they remained almost unchanged for all NPs used. On the contrary, bcl-2 was found down-regulated in every cell line except Fe_3O_4 core Ag shell in HEK293 and Fe_3O_4 core Au shell and Fe_3O_4 HUH7 cells. These results are consistent with the MTT results; HEK293 had the mildest viability reduction and also showed the mildest fold change in gene expression. All the cancer cell lines which had an increased toxicity also showed an analogous fold change in gene expression. These results reveal that cancer cells treated with the hyperthermic NPs used in this study show anti-cancer potency via the caspase cascade and the p53/bcl-2 apoptotic pathway. However, 4T1 cells are p53-null. Thus, the cellular death mechanism is triggered by a p53 independent pathway. Yerlikaya et al [13], showed that a proteasome inhibitor leads to a p53 independent apoptosis in 4T1 p53-null cells. Despite the different stimuli (hyperthermia vs proteasome inhibition) the cellular response was the same: caspase-3 was up-regulated. The latter highlights that, p53-deficient cells can also

perform apoptosis via caspase-3. However further research the underlying mechanisms involved is crucial since in some cancer types p53 is found mutated up to 50% [25]. Additionally, studies have shown contradicting results about the role of pro-apoptotic genes involved in p53-independent apoptosis [13].

Our results are in agreement with other studies in which hyperthermia (not mediated by NPs) results in the apoptotic death of cancer cells [26,27], while two more studies using NP-mediated hyperthermia also support this conclusion [28,29]. Furthermore, one study using hyperthermia on p53 deficient H1299 lung cancer cells showed too, that the underlying mechanism of cellular death is apoptosis [30].

Based on our findings, the NPs we used seem to have specificity towards cancer cells. We deemed that is has to do with the use of tryptophan as a stabilizer and reducing agent. Tryptophan is demonstrated to have rather a positive effect on both cell lines compared to the positive control, especially on cancer cells (data not shown). Thus, the increased metabolism of Trp by cancer cells specifically may be beneficial in order to increase the anti-tumour effect of NPs [31]. However, further research is required to elucidate the p53-independent apoptosis triggered by hyperthermic NPs and to predict the vulnerability of cancer cell types towards a particular hyperthermic NP (Fe_3O_4 $_{core}$ Au $_{shell}$ or Fe_3O_4 $_{core}$ Ag $_{shell}$).

Conclusion

Based on our results, Fe_3O_4 $_{core}$ Au $_{shell}$ (concentrations 400 and 600μg/mL) are the most efficient of the NPs tested to induce cytotoxicity on cancer cells HCT116 and 4T1. On the other hand, Fe_3O_4 $_{core}$ Ag $_{shell}$ (200, 400 and 600) induce cytotoxicity on HUH7 cells; it seems that the endogenous toxicity of Ag works synergistically with hyperthermia. The mechanism of cellular death is apoptosis via the p53/bcl-2/casp-3

pathway for HCT116 and HUH7 cells. 4T1 cells also undergo apoptosis but via a p53-independent pathway.

Experimental

Fe_3O_4 core Ag(Au) shell NPs synthesis

Colloidal solutions of nanocomposites containing iron oxide core and noble metal shell Fe_3O_4 core Ag(Au) shell were obtained via chemical reduction of metal ions (AgNO3, HAuCl4, Merck, Germany) by amino acid tryptophan (Trp, SC12-20120713, China) in the presence of magnetic fluid - suspension of iron oxide Fe_3O_4 in sodium oleate. The synthetic procedure was similar to the previously described.[7] Initial solution of Trp was adjusted to high pH and heated to boiling. Then magnetite was injected followed by silver nitrate (tetrachlorauric acid). The components molar ratio was v(Trp): v(M): v(Fe_3O_4) = 2:1:0,5. Colloid was stirred and heated continuously.

Cell culture

HEK293, HCT116, 4T1 and HUH7 cell lines were grown in DMEM High Glucose culture medium (BioSera) containing 10% FBS, 2 mmol/L glutamine, 100 U/ml penicillin and 100 g/ml streptomycin at 37 ^{o}C. The medium was changed every 48 h and cells were passaged once weekly using standard trypsin-EDTA concentrations. Beginning at passage 38, 32, 41 and 36 respectively, cells were cultured continuously. Cells were frozen in freezing medium containing FBS, 5% DMSO. All cell lines used are adherent. HEK293 cell line was used as control group (non-cancerous cell line) in our experiments.

MTT assay

The MTT Cell Viability Assay measures alterations in cell viability; when metabolic events lead to apoptosis or necrosis, the cell viability is decreased. As a general protocol, 50.000 cells/well were seeded in 24-well plates (Corning-Costar, Corning, NY) and cultured overnight. Three different types of controls, namely: positive, negative and background were used throughout the study. Positive control had cells with culture medium but not exposed to NPs. Negative control had NPs without cells. Background control had culture medium without cells. The cell lines used were treated with 200, 400 and 600µg/mL of Fe_3O_4 core Ag shell, Fe_3O_4 core Au shell and Fe_3O_4 alone for 1 h and then ionized for 15 min. Subsequently, the cells were rinsed once and incubated in 37 oC with 100 µL of serum-free medium containing 0.5 mg/mL MTT. After 1.5 to 2.5 hours, 100µL of SDS-HCl were added to each well, mixed with the thoroughly and incubated for at least 1 hour in 37^{o}C. The optical densities were read at 570nm (reference filter was set at 690nm), using a microplate spectrophotometer (SPECTROstarNano, BMG LABTECH). Absorbances were normalized with respect to the untreated control cultures to calculate changes in cell viability.

Hyperthermia

The hyperthermia session was performed using a water loaded circular waveguide applicator (diameter of 7cm) with an effective aperture of 7cm. [11] HEK293, HCT116, 4T1 and HUH7 cells were incubated for 20min at the temperature of 43 oC. The hyperthermia device was operated as a 433 MHz microwave heating. The microwave device had an omitted power of 100Watts RMS. However, the transmitted power in our case was at the level of 15-20 Watts for 4min [12].

RNA extraction and quantitative real-time RT-PCR

Total RNA extraction (for all three NPs used and for concentration of 400μg/mL) was performed using TRIzol reagent (Thermo Fisher Scientific), according to the manufacturer's instructions. Reverse transcription was performed using the PrimeScript First Strand cDNA Synthesis Kit (TAKARA). The reaction conditions were as follows:

37^{o}C for 30min and 85^{o}C for 5s. The reaction was performed on Thermal Cycler (Kyratec Super Cycler). Assessment of casp-3, bcl-2, p53 and hsp-70 mRNA levels was performed for HCT116, 4T1, HUH7 and HEK293; 4T1 cells are p53 null [13] and as such expression of p53 was not investigated.

Quantitative real-time RT-PCR was conducted on an ABI Prism 7000 apparatus (Applied Biosystems, Foster City, CA, USA). Each cDNA sample was mixed with specific primer sets and PCR master mix (KAPA SYBR FAST qPCR Kit). The levels of genes expression were normalized by subtracting the Ct value of the GAPDH RNA internal control from that of the GOI (gene of interest) ($\Delta Ct=-|CtGOI - CtGAPDH|$). To determine the relative expression of GOI in cancer cells compared to non-cancer cells the $2^{\Delta\Delta Ct}$ model was used, where $\Delta\Delta Ct=\Delta CtGOI-\Delta CtGAPDH$.

Statistical analysis

All statistical analyses were performed using GraphPad version 3.00 (GraphPad Software, San Diego, CA). $p>.05$ was considered significant

Acknowledgements

«This research is co-financed by Greece and the European Union (European Social Fund- ESF) through the Operational Programme «Human Resources Development, Education and Lifelong Learning» in the context of the project “Strengthening Human Resources Research Potential via Doctorate Research” (MIS-5000432), implemented by the State Scholarships Foundation (IKY)»

and National Academy of Sciences of Ukraine through grant of NASU for the research laboratory/group of young scientists of NASU for conducting investigations in priority directions of science and technology development in 2018-2019.

References

1. Silva, A. C.; Oliveira, T. R.; Mamani, J. B.; Malheiros, S. M.; Malavolta L.; Pavon, L. F.; Sibov L. F.; Amaro, E. Jr.; Tannus. A.; Vidoto. E. L.; Martins, M. J.; Santos, R. S.; Gamarra, L. F. *Int J Nanomed* **2011**, *6*, 591-603.

2. Hildebrandt, B.; Wust, P.; Ahlers, O.; Dieing. A.; Sreenivasa, G.; Kerner, T.; Felix, R.; Riess, H. *Crit Rev Oncol Hematol* **2002**, *43* (1), 33-56.

3. Ferrari, M. *Nat Rev Cancer* **2005**, *5* (3), 161-71.

4. Sharma, A.; Goyal, A. K.; Rath, G. *J Drug Target* **2008**, *26* (8), 617-32.

5. Thiesen, B.; Jordan, A. *Int J Hyperthermia* **2008**, *24* (6), 467-74.

6. Kumar, C. S.; Mohammad, F. *Adv Drug Deli Rev* **2011**, *63* (9), 789-808.

7. Mukha, I.; Vityuk, N.; Grodzyuk, G.; Shcherbakov, S.; Lyberopoylou, A.; Efstathopoulos, E.; Gazouli, M. *J Nanosci Nanotechnol* **2017**, *17* (12), 8987-8994.

8. Shmarakov, I.; Mukha, I.; Vityuk N. *Nanoscale Res Lett* **2017**, *12*, 333.

9. Wang, H. Y.; Fu, C. M.; Lee, Y. C.; Lu, P. J. *Mol Cell Biol* **2013**, *33* (24), 4889-4899.

10. Shmarakov, I. O.; Mukha, I. P.; Karavan, V. V.; Chunikhin, O. Y.; Marcheko, M. M.; Smirnova, N. P.; Eremenko A. M. *Nanobiomedicine* **2014**, *1*, 1-10.

11. Vazquez-Muñoz, R.; Borrego, B.; Juárez-Moreno, K.; Garcia-Gracia, M.; Mota, Morales, J. D.; Bogdanchikova, N.; Huerta-Saquero A. *Toxicol Lett* **2017**, *276*, 11-20.

12. Zhang, X.; Li, Y.; Huang, Q.; Wang, H.; Yan, B.; Dewhirst, M. W.; Li, C. Y. *Clin Canc Res* **2003**, *9* (3), 1155-1160.

13. Yang, K. L.; Huang, C. C.; Chi, M. S.; Chiang, H. C.; Wang, Y. S.; Hsia C. C.; Andocs G.; Wang, H.; E.; Chi, K. H. *Oncotarget* **2016**, *7* (51), 84082-84092.

14. Mantso, T.; Vasileiadis, S.; Anestopoulos, I.; Voulgaridou, G. P.; Lampri, E.; Botaitis, S.; Kontomanolis, E. N.; Simopoulos, C.; Goussetis, G.; Franco, R.; Chlichlia, K.; Pappa, A.; Panayiotidis, M. I. *Sci Rep* **2018**, *8*, 10724.

15. Garrido, C.; Brunet, M.; Didelot, C.; Zermati, Y.; Schmitt, E.; Kroemer, G. *Cell Cycle* **2006**, *5* (22), 2592-2601.

16. Tsang, Y. W.; Huang, C. C.; Yang, K. L.; Chi, M. S.; Chiang, H. C.; Wang, Y. S.;Andocs, G.; Szasz, A.; Li, W. T.; Chi, K. H. *BMC cancer* **2015**, *15*, 708.

17. Hassan, M.; Watari, H.; AbuAlmaaty, A.; Ohba, Y.; Sakuragi, N. *Biomed Res Int* **2014**, *2014*, 150845.

18. Zhou, X.; Hao, Q.; Lu, H. *J Mol Biol* **2018**, *11* (4), 293-305.

19. McIlwain, D. R.; Berger, T.; Mak, T. W. *Cold Spring Harb Perspect Biol* **2013**, *5*, a008656.

20. Mello, S. S.; Attardi, L. D. *Curr Opin Cell Biol* **2018**, *51*, 56-72.

21. Um, H. D. *Oncotarget* **2016,** *7*, 5193-203.

22. Yerlikaya, A.; Okur, E.; Ulukaya, E. *Tumor Biol* **2012**, *33*, 1385-1392.

23. Olivier, M.; Hollstein, M.; Hainaut, P. *Cold Spring Harb Perspect Biol* **2010**, *2* (1), a001008.

24. Shellman, Y. G.; Howe, W. R.; Miller, L. A.; Goldstein, N. B.; Pachero, T. R.; Mahajan R. L.; LaRue, S. M.; Norris, D. A. *J Invest Dermatol* **2008**, *128* (4), 949-956.

25. Hou, C. H.; Lin, F. L.; Hou, S. M.; Liu, J. F. *Int H Mol Sci* **2014**, *15* (10),17380-17395.

26. Haghniaz, R.; Umrani, R.; Paknikar, K. *Int J Nanomed* **2015**, *10*, 1609-1623.

27. Ludwig, R.; Teran, F. J.; Teichgraeber, U.; Hilger, I. *Int J Nanomedicine* **2017**, *12*, 1009-1018.

28. Pawlik, A.; Nowak, J. M.; Grzanka, D.; Gackowska, L.; Michalkiewicz, J.; Grzanka, A. *Acta Histochem* **2013**, *115*, 8-15.

29. Prendergast, G. C. *Nature* **2011**, *478* (7368), 192-194.

30. Kouloulias, V. E.; Kouvaris, J. R.; Nikita, K. S.; Golematis, B. C.; Uzunoglu, N. K.; Mystakidoy, K.; Papavasiliou, C.; Vlahos, L. *Int J Hyperthermia* **2002**, *18* (3), 233-252.

31. McWilliams, B.T.; Wang, H.; Binns, V. J.; Curto, S.; Bossmann, S. H.; Prakash, P. *J Funct Biomater* **2017**, *8* (3), E21.